High β Equilibria of Drift Optimized Compact Stellarators

A. S. Ware,[1] S. P. Hirshman,[2] D. A. Spong,[2] L. A. Berry,[2]
A. J. Deisher,[1] G. Y. Fu,[3] J. F. Lyon[2], and R. Sanchez[4]
[1] *University of Montana,Missoula, Missoula, Montana 59812*
[2] *Oak Ridge National Laboratory, Oak Ridge, Tennessee 37831*
[3] *Princeton Plasma Physics Laboratory, Princeton, New Jersey 08543*
[4] *Universidad Carlos III de Madrid, Madrid, Spain*

(Dated: March 19, 2002)

Abstract

Compact stellarator configurations have been obtained with good neoclassical confinement that are stable to both pressure- and current-driven modes for high values of β. These configurations are drift-optimized tokamak-stellarator hybrids with a high shear tokamak-like rotational transform profile and $|B|$ that is approximately poloidally symmetric. The bootstrap current is consistent with the required equilibrium current and, while larger than that in existing stellarators, is typically only a small fraction $(1/3-1/5)$ of that in an equivalent tokamak. Self-consistent bootstrap current profiles have been obtained for plasma pressures in the range $2\% < \beta < 23\%$. These configurations have strong magnetic wells and consequently high interchange stability β limits up to $\beta = 23\%$. Because of the reduced bootstrap current, these configurations are stable to low-n ideal MHD kink modes with no wall stabilization for values of β ($\sim 7-11\%$) significantly larger than in an equivalent advanced tokamak. The combination of high β limits and low bootstrap current in this hybrid device yields a Troyon factor $\beta_N \sim 19$ that is much larger than that for advanced tokamaks.

PACS numbers: 52.55.Hc, 52.55.Fa, 52.55.Tn

Interest in compact stellarators with aspect ratios $A = \langle R \rangle / \langle a \rangle$ in the range $2 < A < 4$ is motivated by the desire to realize an economically sized, high-power-density fusion reactor with little or no recirculating power and freedom from discharge-terminating disruptions. Here $\langle R \rangle$ and $\langle a \rangle$ are the average major and minor radii, respectively, of these noncircular, nonaxisymmetric plasmas. Strong toroidal and helical mode couplings in the equations describing magnetohydrodynamic equilibrium and stability are unique to compact stellarators with very low aspect-ratios. Challenging physics and numerical issues result from the large number of Fourier m-n coefficients (where m and n are the poloidal and toroidal mode numbers) of the magnetic field strength $|B|$ and the metric elements that describe the local geometry of the magnetic surfaces. Lower values of A are expected to lead to higher β limits provided regions of locally unfavorable curvature can be avoided. However, magnetic drifts are enhanced at low A. This, in combination with strong departures from geometric symmetry, leads to enhanced neoclassical transport. Here, $\beta = 2\mu_0 \langle p \rangle / \langle B^2 \rangle$ is the normalized volume-averaged plasma pressure.

Drift optimization [1], which is a technique for aligning bounce-averaged particle drift surfaces with magnetic surfaces, has been successfully applied to suppress this deterioration of particle and energy confinement in compact devices [2]. This approach complements the use of quasi-symmetry, which was applied to the designs of the Helically Symmetric Stellarator [3] and the proposed National Compact Stellarator Experiment [4]. Spong, et al. [5] have analyzed the lower-β properties of one type of drift-optimized compact stellarator: a compact stellarator with low bootstrap current and a stellarator-like rotational transform ($\iota \sim 1/\text{pitch} = 1/q$) profile with low shear that is relatively invariant to changes in β. Shear is the radial change of ι with radius. Here, we describe the higher-β properties of a new, but related, type of compact stellarator: a tokamak-stellarator hybrid with a higher (self-consistent) bootstrap current and $|B|$ exhibiting approximate quasi- poloidal symmetry (qps). This symmetry is defined by $d|B|/d\theta_B \sim 0$, where θ_B is the poloidal Boozer flux angle [6]. Figure 1 shows the last closed flux surfaces for two qps configurations: QPS3, with three field periods ($N = 3$) and high $\beta \sim 15\%$, and QPS2, with two field periods ($N = 2$) and moderate $\beta \sim 5\%$. The colors indicate contours of constant $|B|$. The new configurations have a high-shear ι profile which decreases with plasma minor radius (as in a conventional tokamak) and for which the calculated neoclassical cross-field transport decreases with β because $|B|$ more closely approximates poloidal symmetry. The nonaxisymmetric Fourier

components ($n \neq 0$) of $|B|$ result in a reduced bootstrap current that is only $1/5-1/3$ that of an equivalent tokamak (a torus with the same axisymmetric boundary Fourier components and rotational transform as this qps configuration). The lower current results in MHD stability β limits that are higher than those for the equivalent tokamak: $\beta > 20\%$ for Mercier and ballooning stability and $\beta \sim 11\%$ for vertical and kink stability without a conducting wall.

Unlike classical stellarators, or even some of the quasi-omnigeneous stellarators previously considered, these high-β qps configurations are distinguished by a relatively small external rotational transform arising from coils (typically, $\iota_{\text{coils}} \sim 0.05 - 0.10$). As in a tokamak, the dominant contribution to the rotational transform (away from the plasma edge, at least) is produced by the plasma current. Hence these are stellarator-tokamak hybrid configurations. For the QPS3 configuration in Fig. 1a, ι varies monotonically from 0.4 on axis to 0.1 at the edge, with approximately half of the edge transform due to currents in the external coils. Note that this profile completely avoids the $\iota = 1/2$ and other low-order resonances (where $\iota = M/N$), so internal disruptions should be suppressed. The shear is large so that neoclassical tearing-mode islands should also be suppressed, although not completely stabilized.

The main role of the external stellarator coils in these qps configurations is to substantially reduce (but not eliminate) the bootstrap current. The neoclassical current was computed using an analytic model [7], which was incorporated into an iterative nonlinear stellarator optimization code [5]. The QPS2 and QPS3 configurations were optimized for consistency of the equilibrium and bootstrap currents, so that the required equilibrium plasma current was composed entirely of the bootstrap current associated with the pressure and ι profiles. As previously noted, the bootstrap currents for these cases are lower than that in an equivalent tokamak. Alternatively, the bootstrap current in such a tokamak would be too large to be consistent with these values of ι and β. Therefore, in a tokamak, driven currents would be needed to cancel most of the bootstrap current to achieve equilibrium and stability. Figure 2 shows the profiles of the equilibrium current (green), the computed bootstrap current (blue), and the bootstrap current in an equivalent tokamak (red) as a function of the normalized toroidal flux variable $s \sim (r/a)^2$ for the QPS3 configuration. The reduction in the bootstrap current is due to the approximate quasi- poloidal symmetry of $|B|$. Figure 3 shows contours of $|B|$ in magnetic flux coordinates for QPS3 on the flux surface $\rho = \sqrt{s} = 0.75$. While

the poloidal variation of $|B|$ is small, the components that break the qps are nonnegligible. Exact qps would reduce the bootstrap current by a factor $\sim \iota/N$ (which is comparable to what is computed numerically. This differs from the near-cancellation of toroidal and helical components of current in Wendelstein 7-X [1] and the low-bootstrap-current, quasi-omnigeneous stellarators [5]. Self-consistent bootstrap current profiles have been obtained for plasmas in the range $2\% < \beta < 23\%$. No auxiliary on-axis "seed" current is required to achieve the optimized ι profile. This results from the presence of a trapped particle population at the magnetic axis which is created by the $m = 0, n \neq 0$ components of $|B|$.

The bootstrap current is proportional to the Onsager transport coefficient (L_{31}), which is shown for the QPS3 configuration in Figure 4 as a function of ν/v for several values of β (but with fixed shape and rotational transform profile). Here, ν is the collision frequency and v is the particle speed. A neoclassical transport code [8] was used to solve the drift kinetic equation in magnetic flux coordinates and stellarator geometry. The computed coefficient L_{31} decreases as β increases. This results in the bootstrap current, which is proportional to the product of L_{31} and β, becoming nearly independent of β at higher values of β. This is a unique form of configurational invariance: the nonzero bootstrap current and, hence, the ι profile remain nearly constant as β increases. Therefore, new low-order rational resonant surfaces do *not* enter the plasma as β increases (so the magnetic surfaces should be configurationally robust), and a simple vertical field should suffice to compensate for outward radial shifts of the flux surfaces due to the Pfirsch-Schlüter current.

The presence of a finite bootstrap current distinguishes these qps configurations from previous compact stellarators which have very low bootstrap current and results in reductions of both the helical curvature and the connection length. Both of these effects contribute to the higher ballooning stability β limits that are computationally observed. Infinite-n ballooning mode stability was analyzed using the numerically- efficient ballooning code COBRA [9], which was also incorporated into the stellarator optimization code. The ballooning stability β limit for these qps configurations was found to be very high. By optimizing the shape of the last closed magnetic flux surface, together with the pressure profile, for targeted values of β, we obtained ballooning-stable configurations with self-consistent bootstrap current for plasmas in the range $2\% < \beta < 23\%$. For the QPS3 high-β configurations, decreasing β with fixed shape and ι profile resulted in ballooning-unstable configurations. Figure 5 shows ballooning growth rates across the minor radius of QPS3 as β is varied. As β is lowered

to 13%, a single surface near the edge becomes unstable. The edge region of instability broadens and the maximum growth rate becomes larger as β is lowered to 9%. As β is further lowered to 3%, the edge region of instability increases, but the peak growth rate decreases. If β is lowered even further, the region of instability spreads over the majority of the plasma cross section. The plasma finally becomes ballooning stable again for $\beta < 0.5\%$. This stability behavior as a function of β indicates that these plasmas are in the second-stable ballooning regime for $\beta > 13\%$. We note that relatively small shape and profile modifications can produce stable plasmas at all values of $\beta < 23\%$ for QPS3. Future work on the QPS3 configurations will examine the unresolved issue of accessing high-β regimes from low β.

These configurations have good Mercier (local interchange) stability properties resulting from a magnetic well over the entire plasma cross section, with the exception of a few isolated resonances where ι takes on low-order rational values. The resulting localized interchange instabilities could lead to lower β values if they occur near the plasma edge and if they proliferate over a range of radii. The QPS3 ($\beta = 15\%$) configuration is Mercier stable except near the $\iota = 1/5$ and $\iota = 5/12$ resonances, which occur well inside the plasma. The QPS2 ($\beta = 5\%$) configuration is Mercier stable except near the $\iota = 3/8$ resonance.

The presence of a nonzero net plasma current in these compact stellarators makes them potentially susceptible to vertical and kink modes. Stability to these modes was assessed using the Terpsichore code [10] after completion of the other optimizations. In spite of its nonzero plasma current and high $\beta \sim 15\%$, the QPS3 configuration was stable to vertical modes and only weakly unstable to an external kink mode (with normalized growth rate $\gamma\tau_A \sim 2 \times 10^{-2}$, where τ_A is the Alfvén time). Keeping the same shape but scaling β down to $\sim 11\%$ (keeping ι fixed) completely stabilized the kink mode. At this value of β, the Troyon factor, $\beta_N \equiv \beta\,(\%)\,[< a > (\mathrm{m})\, B\,(\mathrm{T})\,/I\,(\mathrm{MA})]$, reaches a value of $\beta_N = 19$, which is significantly larger than $\beta_N \sim 3$ for kink stability in an equivalent tokamak with no wall stabilization. This stability at high β to the most deleterious modes (for tokamaks) is achieved by the nonaxisymmetric components in $|B|$, which reduce the self-consistent bootstrap current to a small fraction of that for a tokamak with a similar ι and shape.

The QPS2 configuration is computed to have a lower stability β threshold for the vertical mode than QPS3. However, by either increasing the fraction of external rotational transform or reducing the axisymmetric elongation [11], related configurations that were stable to the

vertical mode up to $\beta \sim 5\%$ could be achieved. Stabilization of these low-n macroscopic modes should also be possible, either through current profile tailoring (reducing the pressure gradient, and hence the bootstrap current, near the plasma edge) or through dynamic feedback provided by suitable external coils, as is done for shaped tokamaks. Future development of the QPS2 configurations will incorporate these low- n MHD stability calculations into the iterative stellarator optimization process.

Neoclassical confinement is a concern for compact stellarator configurations because of the residual nonsymmetry of $|B|$. Using both drift-orbit and enhanced quasi-poloidal symmetry optimization targets has led to the present configurations, which have adequate levels of neoclassical confinement. Neoclassical ion and electron confinement times were calculated using a Monte Carlo approach [5]. For a QPS3 configuration scaled down to the size and field strength ($\langle R \rangle = 0.86$ m, $\langle B \rangle = 1T$) of a near-term experiment, the predicted global neoclassical energy confinement time ($\tau_{E_{neo}}$) is 14 ms for a low-collision-frequency, hot-electron plasma and 58 ms for a moderate-collision-frequency plasma with equal ion and electron temperatures. A comparison of these times with the confinement time predicted by the ISS95 empirical scaling law [12] yields $\tau_{E_{neo}}/\tau_{E_{ISS95}} = 1.4 - 3.6$ for expected values of the radial electric field. Under these conditions, the neoclassical losses are tolerable in the sense that anomalous processes should dominate the thermal transport. The kinetic transport code DKES [8] was used within the iterative stellarator optimization process to further improve $\tau_{E_{neo}}$ for these plasmas, after a promising region of configurations had been identified. A factor of 2 increase in $\tau_{E_{neo}}$ was obtained by minimizing the local radial particle and energy transport at several surfaces without sacrificing ballooning and kink stability.

An attractive feature of these configurations is that as β increases, the alignment of particle drift and magnetic flux surfaces improves, as in Wendelstein 7-X [1]. The previously mentioned configurational invariance that is achieved in these devices results from the improved degree of qps with increasing β. High β also results in a diamagnetic depression (magnetic well) of the $|B|_{0,0}$ component of the magnetic field. The resulting increased radial gradient of $|B|_{0,0}$ improves the confinement of energetic trapped particles by increasing their poloidal drift, analogous to the way that the ambipolar electric field improves the confinement of thermal particle orbits [13]. A consequence of this is that alpha particle confinement improves with increasing β [5]. At $\beta = 23\%$, the level of alpha energy losses are $\sim 12\%$.

In summary, we have found compact, quasi-poloidally symmetric stellarators with high

MHD stability β limits and good neoclassical confinement. The rotational transform in these hybrid cofigurations is produced primarily by a self-consistent bootstrap current. The nonaxisymmetric components of $|B|$ yield a bootstrap current lower than that in an axisymmetric device, which leads to good MHD stability properties without need for a conducting wall. The neoclassical confinement improves with increasing β, leading to a new form of configurational invariance in these stellarators.

The authors thank D. B. Batchelor for his encouragement throughout this project, D. Strickler for making some preliminary calculations of coils for these configurations, and M. B. Nestor for her diligent editorial comments. This research was supported by the U.S. Department of Energy under Grant No. DE-FG 03-97ER54423 at the University of Montana and under contract DE-AC05-00OR22725 at Oak Ridge National Laboratory, managed by UT-Battelle, LLC.

---

[1] G. Grieger et al., Plasma Physics and Controlled Nuclear Fusion Research, Proceedings 13th International Conference, Washington, 1990, Vol. 3, p. 525 (International Atomic Energy Agency, Vienna, 1991).

[2] S. P. Hirshman et al., Phys. Plasmas **6**, 1858 (1999).

[3] D. T. Anderson, et al., J. Plasma Fusion Res. **1**, 49 (1998).

[4] G. H. Neilson et al., Phys. Plasmas **7**, 1911 (2000).

[5] D. A. Spong et al., Nucl. Fusion **41**, 711 (2001).

[6] A. H. Boozer, Phys. Fluids **23**, 904 (1980).

[7] K.C. Shaing et al., Phys. Fluids B1 **148** (1989).

[8] W. I. van Rij and S. P. Hirshman, Phys. Fluids B **1**, 563 (1989).

[9] R. Sanchez et al., J. Comp. Phys. **161**, 576 (2000).

[10] W. A. Cooper, D. B. Singleton, and R. L. Dewar, Phys. Plasmas **3**, 275 (1996).

[11] G. Y. Fu, Phys. Plasmas **7**, 1079 (2000).

[12] U. Stroth et al., Nucl. Fusion **36**, 1063 (1996).

[13] M. Yokoyama et al., Nucl. Fusion **40**, 261 (2000).

FIGURE CAPTIONS

Figure 1. Last closed flux surface for (a) QPS3, with three field periods, $A = 3.7$, $\beta = 15\%$, and (b) QPS2, with two field periods, $A = 2.7$, $\beta = 5\%$. Color indicates the variation in $|B|$.

Figure 2. Profiles of $\langle J \cdot B \rangle$ for QPS3 shown in Fig. 1a. Shown are the equilibrium current (green), bootstrap current (blue), and bootstrap current in an equivalent tokamak (red). The currents are antiparallel to the magnetic field. Thus, the magnitude of the current decreases towards the top.

Figure 3. Contours of $|B|$ in Boozer coordinates on the $\rho = 0.75$ flux surface for QPS3 shown in Fig. 1a. Blue contours indicate $|B| < 1$ T, purple contours indicate $|B| > 1$ T, and red lines indicate the direction of magnetic field lines.

Figure 4. DKES L_{31} bootstrap transport coefficient for QPS3 as a function of ion collisional frequency parameter for three values of β.

Figure 5. Ballooning growth rate as a function of β for QPS3.

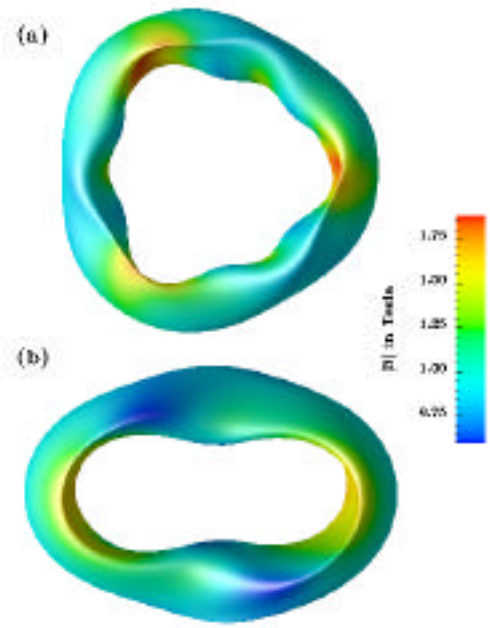

FIG. 1: Last closed flux surface for (a) QPS3, with three field periods, $A = 3.7$, $\beta = 15\%$, and (b) QPS2, with two field periods, $A = 2.7$, $\beta = 5\%$. Color indicates the variation in $|B|$.

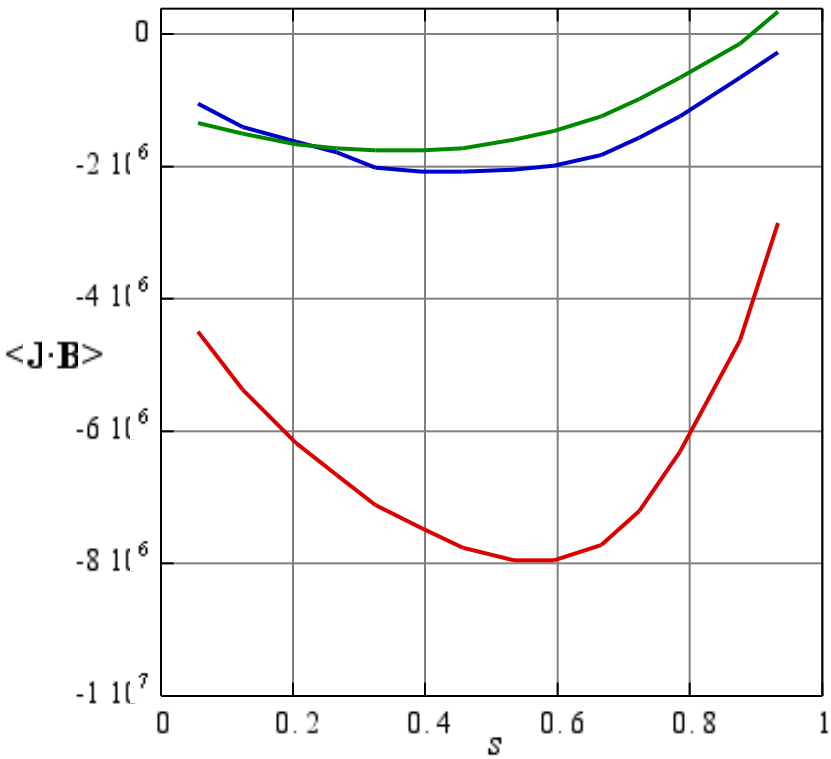

FIG. 2: Profiles of $\langle J \cdot B \rangle$ for QPS3 shown in Fig. 1a. Shown are the equilibrium current (green), bootstrap current (blue), and bootstrap current in an equivalent tokamak (red). The currents are antiparallel to the magnetic field. Thus, the magnitude of the current decreases towards the top.

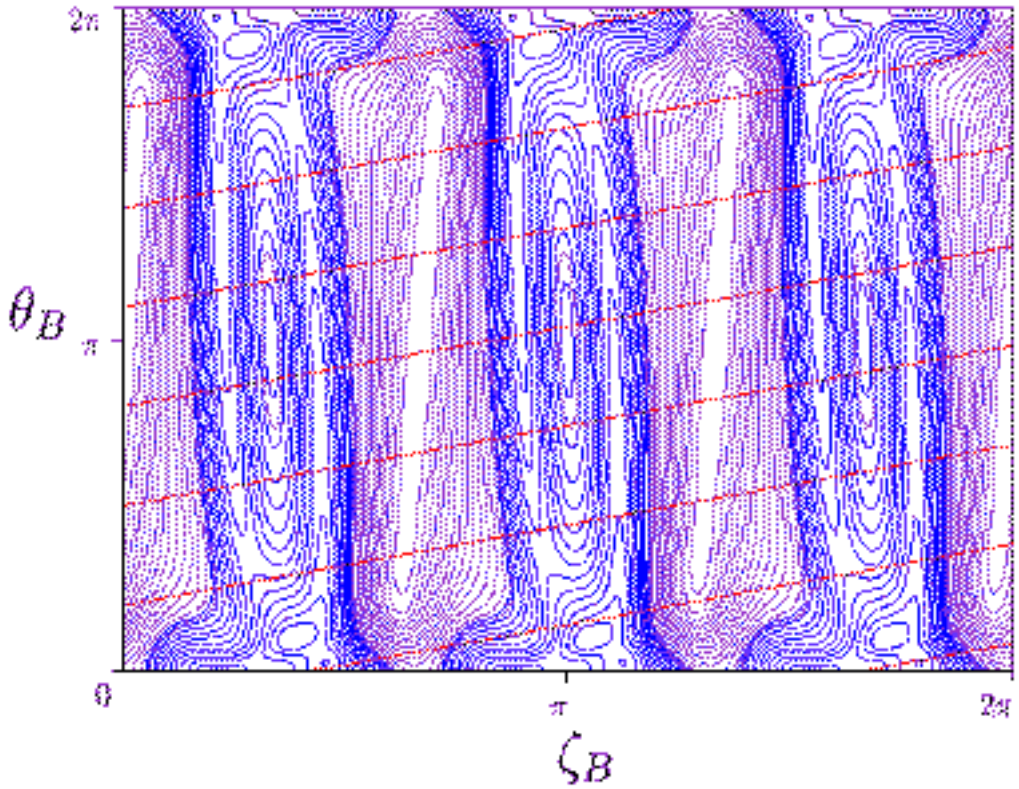

FIG. 3: Contours of $|B|$ in Boozer coordinates on the $\rho = 0.75$ flux surface for QPS3 shown in Fig. 1a. Blue contours indicate $|B| < 1$ T, purple contours indicate $|B| > 1$ T, and red lines indicate the direction of magnetic field lines.

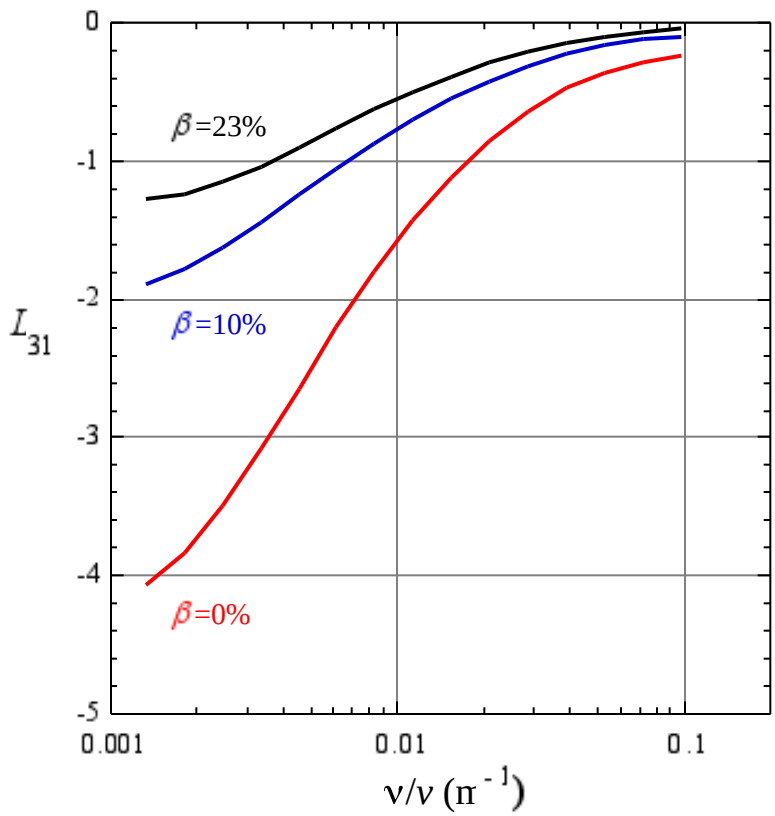

FIG. 4: DKES L_{31} bootstrap transport coefficient for QPS3 as a function of ion collisional frequency parameter for three values of β.

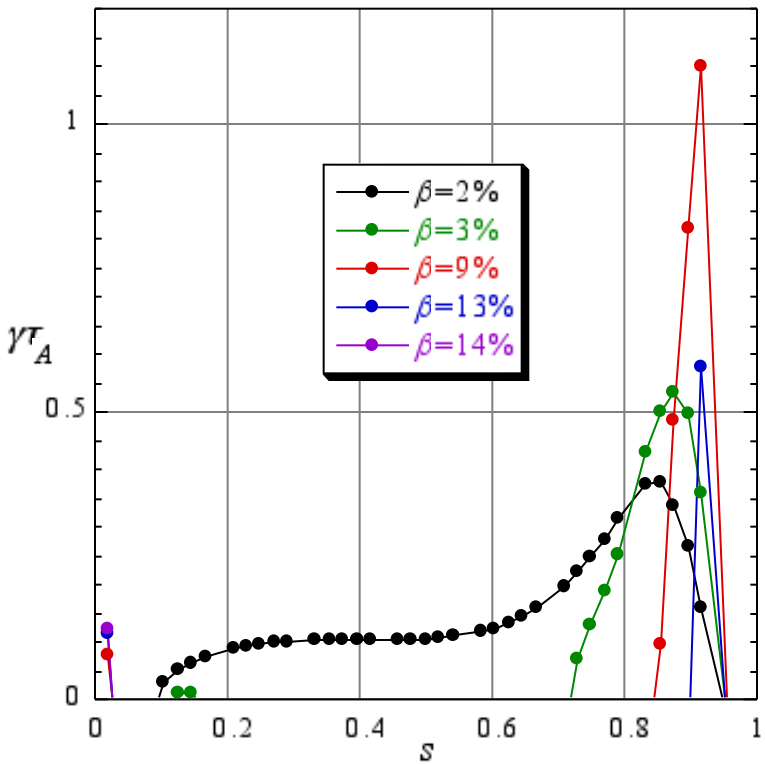

FIG. 5: Ballooning growth rate as a function of β for QPS3.